JST: Smart Systems and Devices
Volume 35, Issue 2, May 2025, 001-008

Optimal Design of Proportional-Differential Controller in Active Control of Suspension Systems Using the Balancing Composite Motion Optimization Algorithm

Hai-Le Bui[1*], Thi-Thoa Mac[1], Van-Quyen Nguyen[1], Ngoc-An Tran[2], Tung-Anh Le[3], Quy-Cao Tran[4], Sy-Tai Nguyen[5]
[1] *Hanoi University of Science and Technology, Ha Noi, Vietnam*
[2] *Vietnam Maritime University, Hai Phong, Vietnam*
[3] *Vietnam Maritime Administration, Ha Noi, Vietnam*
[4] *Phuong Dong University, Ha Noi, Vietnam*
[5] *Vietnam National Institute of Occupational Safety and Health, Ha Noi, Vietnam*
[*] *Corresponding author email: le.buihai@hust.edu.vn*

Abstract

The study presents a simple way to optimally design a Proportional-Differential (PD) controller and apply it to the vibration control of a quarter car model's active suspension system. First, the optimization objectives are determined, including minimizing the vehicle body acceleration and the suspension deflection. The tyre deflection and road holding constraints are also considered. Next, the variables, including the components in the gain vector of the PD controller, are optimized using the Balancing Composite Motion Optimization (BCMO) algorithm. Different controller configurations, according to the two above optimization objectives, are simulated to verify the performance of the controllers for the nominal system and for the system when its mass and stiffness are varied. An H_∞ controller in a reputable published study is also included for comparison. The simulation results show the proposed PD controllers' high control efficiency and robustness, especially the PD controller, which is based on minimizing the vehicle body's acceleration.

Keywords: Active suspension, BCMO, PD controller.

1. Introduction

The problem of controlling the vibration of structures is often to reduce or eliminate unwanted vibrations. Therefore, this problem has received the attention of many researchers [1-5].

Among control structures, active suspension systems of transport vehicles also need due attention because the safety and comfort of cars need to be continuously improved to serve passengers and luggage [6-8].

Many different control algorithms have been applied to the field of structural vibration control in general and vibration control of active suspension systems in particular [1-8]. Among these controllers, the Proportional-Differential (PD) controller is commonly used because it has many advantages, such as simplicity, high efficiency, and ease of optimization. Determining the parameters of PD controllers can be done by trial and error methods or by using tuning tools of specialized software.

The Balancing Composite Motion Optimization (BCMO) is a recently published herding-based optimization algorithm [9]. This algorithm has many advantages, such as not requiring algorithm parameters, being simple to use, fast convergence, etc.

For the above reasons, this study presents a simple approach to optimally design a PD controller using the BCMO algorithm and applies it to vertical vibration control of an active suspension system of a quarter car model.

2. The Active Suspension Model

Consider the active suspension of a quarter car model, as shown in Fig. 1 [10, 11].

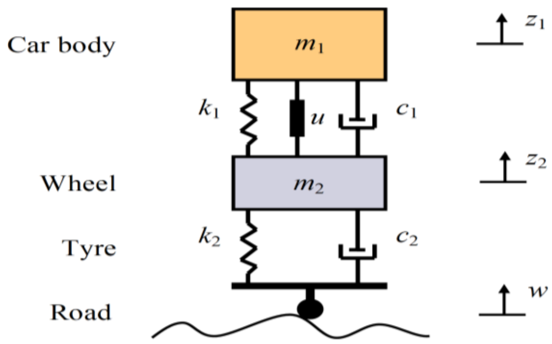

Fig. 1. The active suspension system

ISSN 2734-9373
https://doi.org/10.51316/jst.182.ssad.2025.35.2.1
Received: Oct 26, 2024; revised: Jan 16, 2025
accepted: Jan 16, 2025

In this model, the mass, stiffness, and damping coefficient of the vehicle body and the wheel are m_1, m_2, k_1, k_2, c_1, and c_2, respectively. The car body and the wheel displacements are z_1 and z_2. The road profile is denoted w.

The system's Lagrange equations are as follows:

$$\begin{aligned} &\frac{d}{dt}\left(\frac{\partial T}{\partial \dot{z}_1}\right)-\frac{\partial T}{\partial z_1}=-\frac{\partial \Pi}{\partial z_1}-\frac{\partial \Phi}{\partial \dot{z}_1}+Q_{z_1}^{*} \\ &\frac{d}{dt}\left(\frac{\partial T}{\partial \dot{z}_2}\right)-\frac{\partial T}{\partial z_2}=-\frac{\partial \Pi}{\partial z_2}-\frac{\partial \Phi}{\partial \dot{z}_2}+Q_{z_2}^{*} \end{aligned} \tag{1}$$

where:

$$\begin{aligned} &T=\frac{1}{2}m_1\dot{z}_1^2+\frac{1}{2}m_2\dot{z}_2^2 \\ &\Pi=\frac{1}{2}k_1\left(z_1-z_2\right)^2+\frac{1}{2}k_2\left(z_2-z_r\right)^2 \\ &\Phi=\frac{1}{2}c_1\left(\dot{z}_1-\dot{z}_2\right)^2+\frac{1}{2}c_2\left(\dot{z}_2-\dot{z}_r\right)^2 \\ &Q_{z_1}^{*}=u;Q_{z_2}^{*}=-u \end{aligned} \tag{2}$$

Hence,

$$\begin{aligned} &\frac{\partial T}{\partial \dot{z}_1}=m_1\dot{z}_1 \Rightarrow \frac{d}{dt}\left(\frac{\partial T}{\partial \dot{z}_1}\right)=m_1\ddot{z}_1 \\ &\frac{\partial T}{\partial z_1}=0 \\ &\frac{\partial \Pi}{\partial z_1}=k_1\left(z_1-z_2\right) \\ &\frac{\partial \Phi}{\partial \dot{z}_1}=c_1\left(\dot{z}_1-\dot{z}_2\right) \end{aligned} \tag{3}$$

$$\begin{aligned} &\frac{\partial T}{\partial \dot{z}_2}=m_2\dot{z}_2 \Rightarrow \frac{d}{dt}\left(\frac{\partial T}{\partial \dot{z}_2}\right)=m_2\ddot{z}_2 \\ &\frac{\partial T}{\partial z_2}=0 \\ &\frac{\partial \Pi}{\partial z_2}=-k_1\left(z_1-z_2\right)+k_2\left(z_2-z_r\right) \\ &\frac{\partial \Phi}{\partial \dot{z}_2}=-c_1\left(\dot{z}_1-\dot{z}_2\right)+c_2\left(\dot{z}_2-\dot{z}_r\right) \end{aligned} \tag{4}$$

Therefore, the motion equations of the system are as follows:

$$\begin{aligned} m_1\ddot{z}_1 &=-k_1\left(z_1-z_2\right)-c_1\left(\dot{z}_1-\dot{z}_2\right)+u \\ m_2\ddot{z}_2 &=k_1\left(z_1-z_2\right)-k_2\left(z_2-z_r\right) \\ &\quad +c_1\left(\dot{z}_1-\dot{z}_2\right)-c_2\left(\dot{z}_2-\dot{z}_r\right)-u \end{aligned} \tag{5}$$

The system's state vector is:

$$X=\begin{bmatrix} z_1 \\ z_2 \\ \dot{z}_1 \\ \dot{z}_2 \end{bmatrix} \tag{6}$$

For this active suspension system, the goals and constraints are as follows [10]:

- Minimize the vehicle body acceleration:

$$\left|\ddot{z}_1\right| \rightarrow \min \tag{7}$$

- Minimize the suspension deflection:

$$\left|z_1-z_2\right| \rightarrow \min \tag{8}$$

- Minimize the tyre deflection:

$$\left|z_2-z_r\right| \rightarrow \min \tag{9}$$

- The constraint on the road holding:

$$\frac{k_2\left(z_2-z_r\right)}{g\left(m_1+m_2\right)}<1 \tag{10}$$

The gravitational acceleration g is 9.81 m/s^2.

- The constraint on the actuator limitation (u_{max} is the actuator's maximum control force):

$$\left|u\right| \le u_{max} \tag{11}$$

3. Control Design

The operating diagram of the suspension system using the PD controller is plotted in Fig. 2, where K is the gain vector of the PD controller as follows:

$$K=\begin{bmatrix} k_{P1} & k_{P2} & k_{D1} & k_{D2} \end{bmatrix} \tag{12}$$

Hence, k_{P1} and k_{P2} are coefficients for proportional variables, while k_{D1} and k_{D2} are coefficients for differential variables.

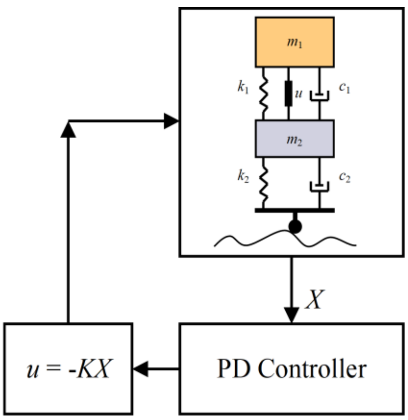

Fig. 2. The operating diagram of the system

The problem of optimal design of the PD controller for the active suspension system, as shown in Fig. 1, is presented with design variables, objective functions, and constraints as following.

- Design variables include four parameters of the gain vector K (k_{P1}, k_{P2}, k_{D1}, and k_{D2}).

- Objective functions are formulas (7) and (8).

- As constraints, in addition to the above constraints in (9) and (10), (8) is converted into the following form:

$$\left|z_2 - z_r\right| \le z_{2r\max} \tag{13}$$

In which $z_{2r\max}$ is a given value.

4. Numerical Simulations

Consider a suspension system with the following parameters [10]: $m_1 = \alpha\times320$ kg, $m_2 = 40$ kg, $k_1 = 18000$ N/m, $k_2 = \beta\times200000$ N/m, $c_1 = 1000$ Ns/m, and $c_2 = 10$ Ns/m, where α and β are real numbers taking on the values 0.9, 1, or 1.1. The road surface profile w has a bump shape [10]:

$$w(t) = \begin{cases} \dfrac{A}{2}\left(1-\cos\left(\dfrac{2\pi V}{L}t\right)\right), \text{if } 0 \le t \le \dfrac{L}{V} \\ 0, \text{if } t > \dfrac{L}{V} \end{cases} \tag{14}$$

where $L = 5$ m and $A = 0.08$ m are the length and height of the bump, respectively. The vehicle's speed V is 12.5 m/s (45 km/h). So,

$$\dot{w}(t) = \begin{cases} 0.2\pi\sin(5\pi t), \text{if } 0 \le t \le 0.4\text{s} \\ 0, \text{if } t > 0.4\text{s} \end{cases} \tag{15}$$

The maximum allowable values of the suspension deflection (SD), the tyre deflection (TD), and the control force are given as [10]: $z_{12\max} = 0.1$ m, $z_{2r\max} = 0.01764$ m, and $u_{\max} = 2500$ N.

The PD controller is optimized according to the objective functions in (7) and (8) and they are denoted as PDa and PDd, respectively, with their gain vectors K_a and K_d. The results of the optimization problem for the gain vectors K_a and K_d are as follows:

K_a = [-12917.37   9414.65   700.94   522.77]

K_d = [-14104.33   12258.64   964.89   -712.78]

In this study, the simulation results of the H_∞ controller (denoted as Hinf) in [10] are also compared in this section. The Hinf's control force is calculated as follows [10]:

$$u = K_i \begin{bmatrix} z_1 - z_2 \\ z_2 - z_r \\ \dot{z}_1 \\ \dot{z}_2 \end{bmatrix} \tag{16}$$

The gain vector K_i is as follows [10]:

K_i = [10098   49655   -1896   909]

First, the simulations are performed with the nominal system ($\alpha = \beta = 1$). Let the relative SD and TD be the ratio between SD and TD to their maximum allowable values, respectively. The relative tyre force (TF) is the ratio in (10). The time responses of the body acceleration, the relative SD, the relative TD, the relative TF, and the control force are shown in Fig. 3. The symbol UC corresponds to the uncontrolled case.

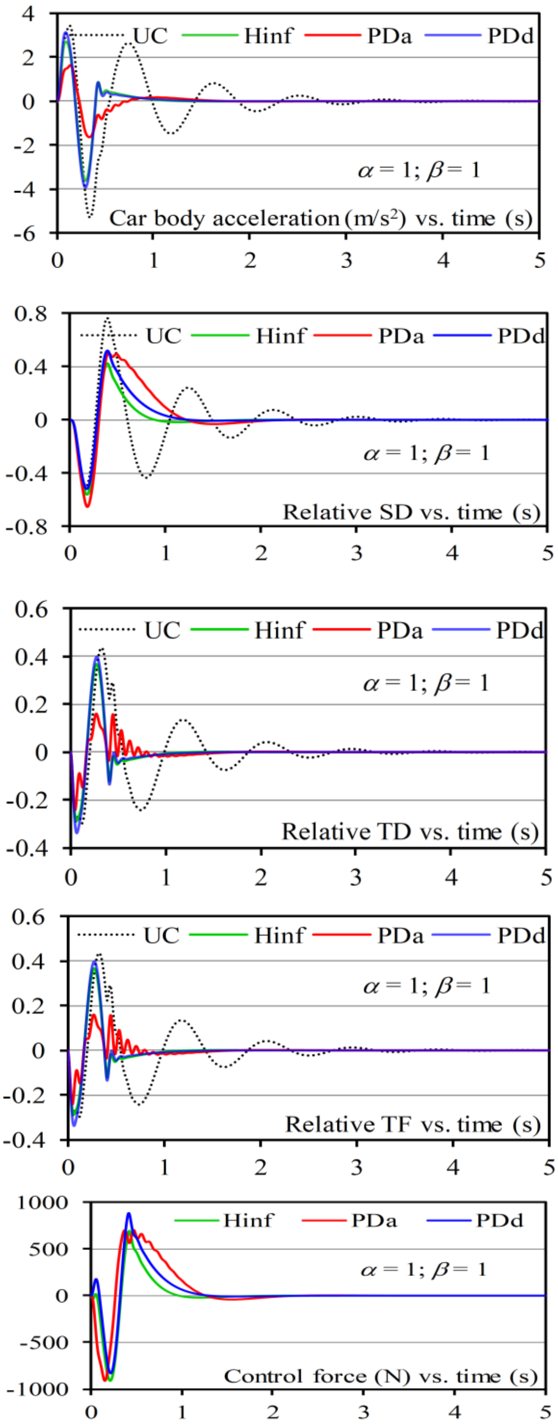

Fig. 3. The system's time responses in the case of $\alpha = \beta = 1$, $V = 12.5$ m/s

The vehicle body mass (m_1) and tyre stiffness (k_2) may change in actual use. Therefore, simulations for different values of α and β are also performed. The results of these simulations are shown in Fig. 4 to Fig. 7 with other pairs of α and β values (V = 12.5 m/s).

The results in Fig. 4 to Fig. 7 when V = 12.5 m/s show that the controllers meet the control objectives, i.e., reduce vehicle body acceleration and suspension deflection compared to the uncontrolled case. At the same time, the controllers are robust to changes in the mass and stiffness parameters of the suspension system.

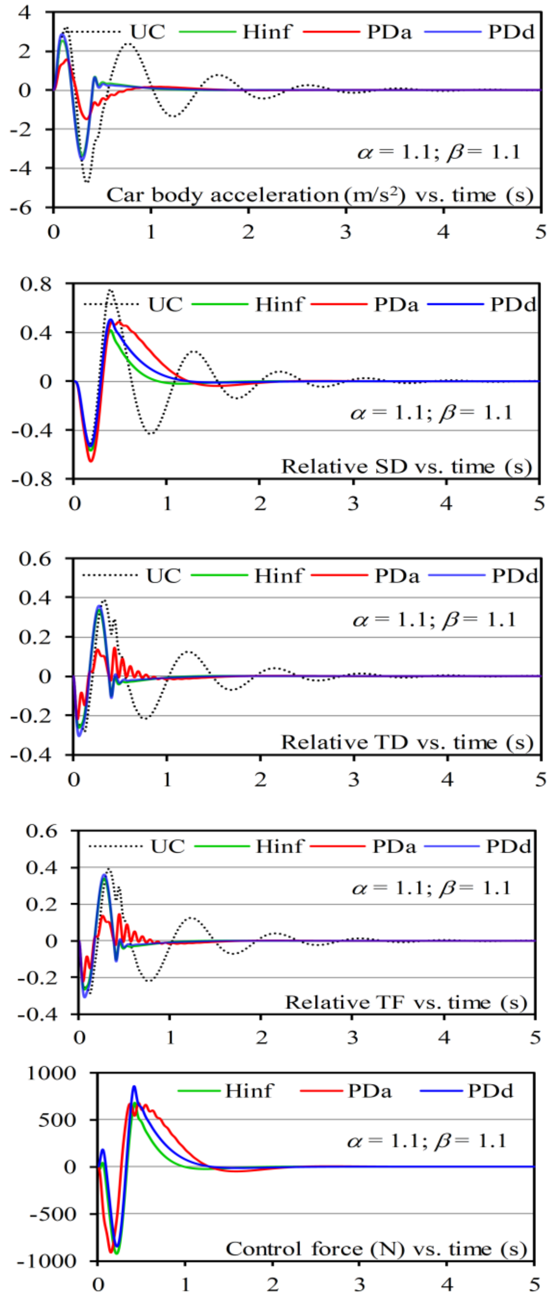

Fig. 4. The system's time responses in the case of α = 1.1 and β = 1.1, V = 12.5 m/s

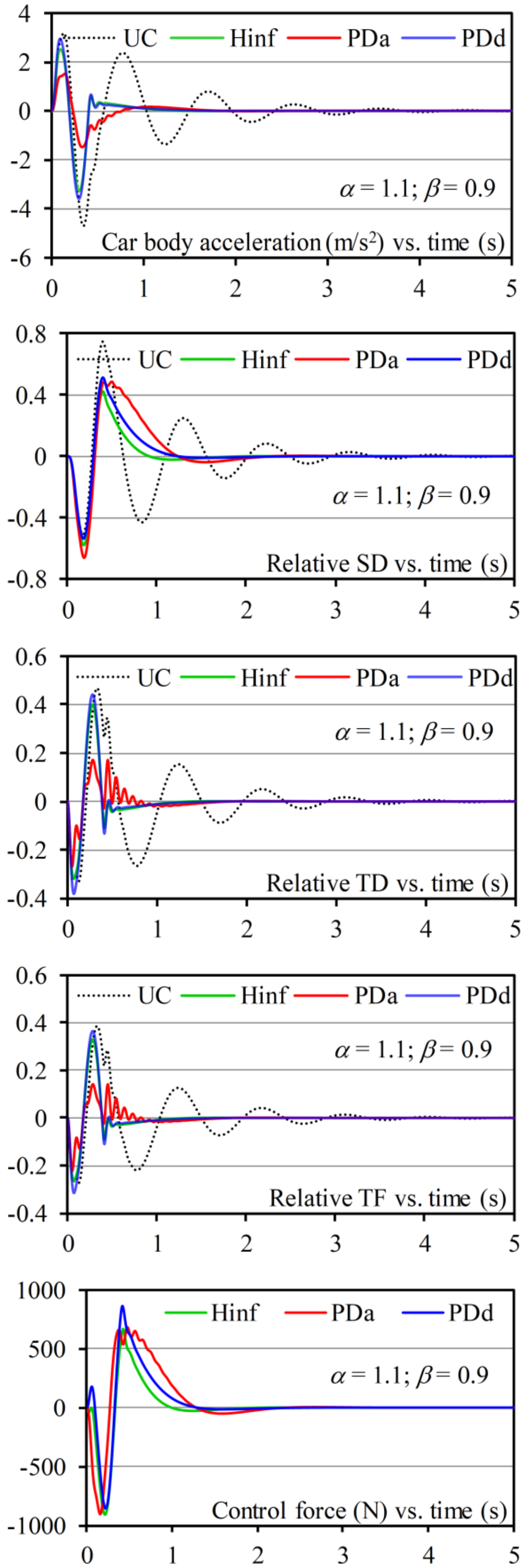

Fig. 5. The system's time responses in the case of α = 1.1 and β = 0.9, V = 12.5 m/s

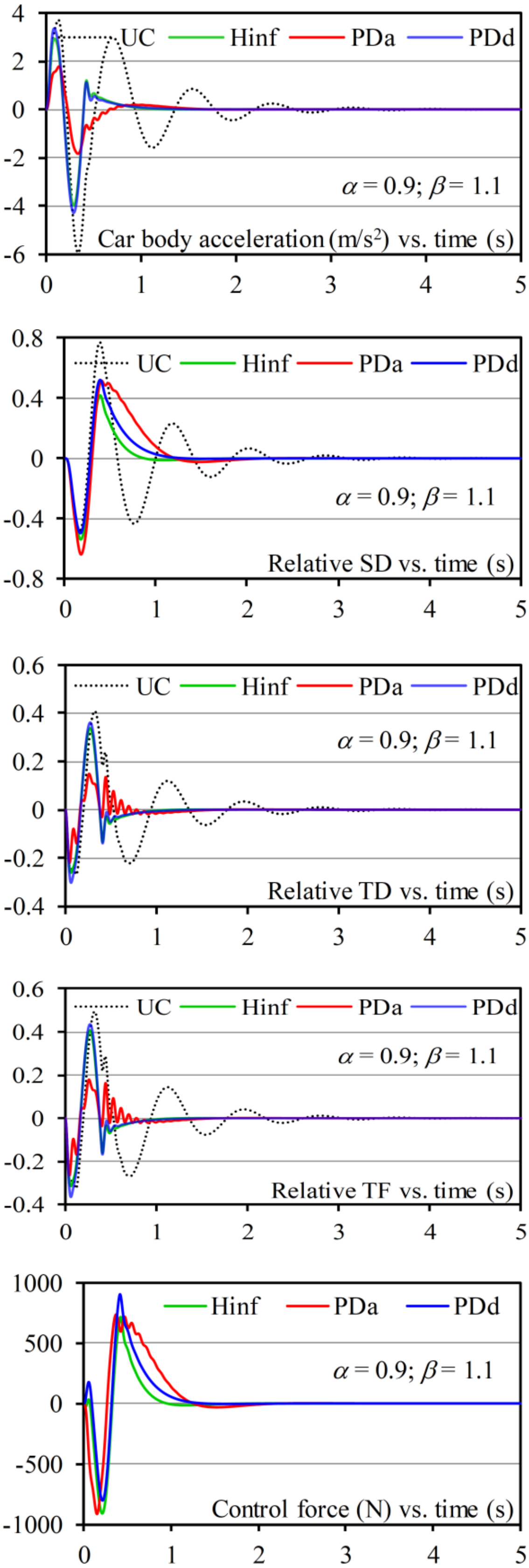

Fig. 6. The system's time responses in the case of $\alpha = 0.9$ and $\beta = 1.1$, $V = 12.5$ m/s

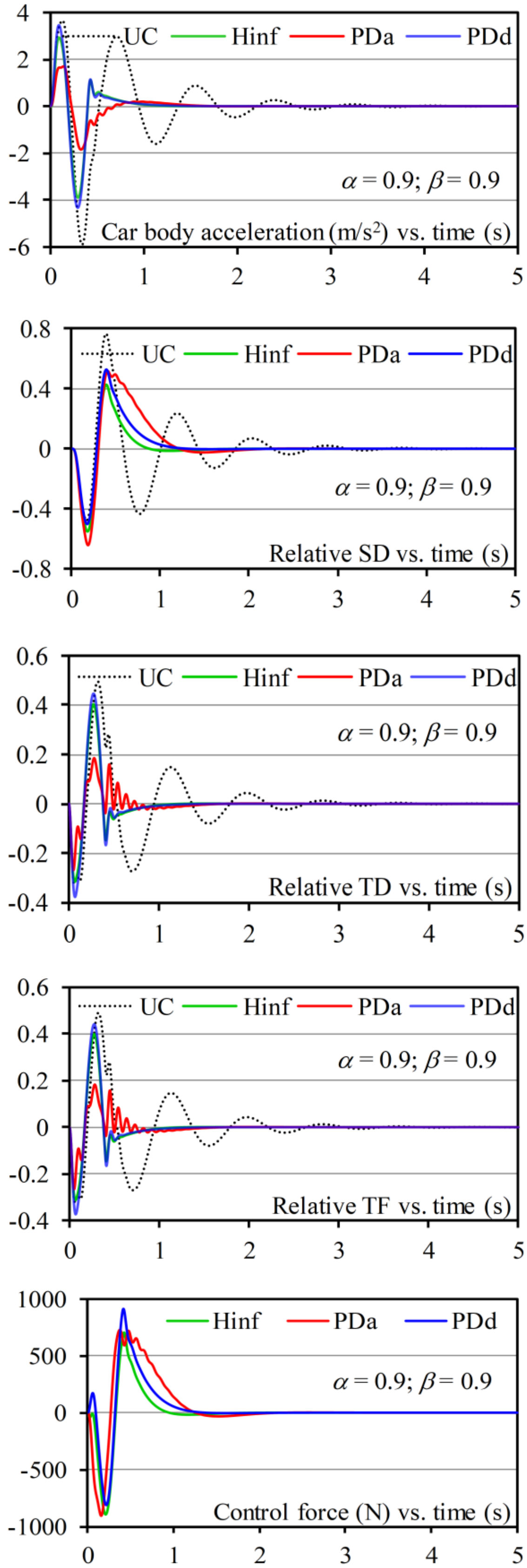

Fig. 7. The system's time responses in the case of $\alpha = 0.9$ and $\beta = 0.9$, $V = 12.5$ m/s

Additionally, the relative SD, the relative TD, the relative TF, and the control force all satisfy their constraints.

The variation (%) of peak values of vehicle body acceleration ($\ddot{z}_1$), SD, TD of Hinf, PDa, and PDd compared to those of the uncontrolled case, and peak value of control force u of PDa and PDd compared to that of Hinf is listed in Table 1.

Table 1a. The variation (%) of peak values of the vehicle body acceleration, SD, TD, and control force criteria (α = 1, β = 1, V = 12.5 m/s)

Criteria	Hinf	PDa	PDd
$\ddot{z}_1$	-31.67	-69.02	-25.90
SD	-26.54	-14.50	-32.00
TD	-15.78	-44.45	-8.82
u	0	0.06	-3.08

Table 1b. The variation (%) of peak values of the vehicle body acceleration, SD, TD, and control force criteria (α = 1.1, β = 1.1, V = 12.5 m/s)

Criteria	Hinf	PDa	PDd
$\ddot{z}_1$	-29.50	-67.03	-25.14
SD	-24.68	-12.80	-29.33
TD	-13.24	-43.26	-7.86
u	0	-1.46	-7.70

Table 1c. The variation (%) of peak values of the vehicle body acceleration, SD, TD, and control force criteria (α = 1.1, β = 0.9, V = 12.5 m/s)

Criteria	Hinf	PDa	PDd
$\ddot{z}_1$	-30.46	-67.99	-23.63
SD	-22.51	-11.43	-28.18
TD	-14.40	-42.44	-5.59
u	0	-0.37	-5.14

Table 1d. The variation (%) of peak values of the vehicle body acceleration, SD, TD, and control force criteria (α = 0.9, β = 1.1, V = 12.5 m/s)

Criteria	Hinf	PDa	PDd
$\ddot{z}_1$	-33.17	-69.11	-28.00
SD	-30.11	-17.19	-32.45
TD	-17.54	-46.22	-11.82
u	0	0.49	-0.85

Table 1e. The variation (%) of peak values of the vehicle body acceleration, SD, TD, and control force criteria (α = 0.9, β = 0.9, V = 12.5 m/s)

Criteria	Hinf	PDa	PDd
$\ddot{z}_1$	-33.98	-68.64	-26.68
SD	-28.11	-16.21	-31.20
TD	-18.65	-45.75	-9.96
u	0	1.30	1.92

In simulation cases when V = 12.5 m/s, the PDa controller gives outstandingly good results for vehicle body acceleration and the relative TD and the relative TF indicators compared to the remaining controllers. The PDd controller provides the best deflection criterion results for the suspension system. The maximum control force of the controllers is approximately equal.

The above simulation results are for the case where the vehicle's speed is 12.5 m/s. Next, the controllers' effectiveness continues to be validated as the vehicle's speed changes.

The variation (%) of peak values of vehicle body acceleration ($\ddot{z}_1$), SD, TD of Hinf, PDa, and PDd compared to those of the uncontrolled case, and peak value of control force u of PDa and PDd compared to that of Hinf when V = 10 m/s and 15 m/s (α = 1, β = 1) is shown in Table 2 and Table 3, respectively.

Table 2. The variation (%) of peak values of the vehicle body acceleration, SD, TD, and control force criteria (α = 1, β = 1, V = 10 m/s)

Criteria	Hinf	PDa	PDd
$\ddot{z}_1$	-45.23	-69.63	-40.56
SD	-36.20	-23.31	-29.93
TD	-36.50	-64.40	-31.65
u	0	1.92	11.82

Table 3. The variation (%) of peak values of the vehicle body acceleration, SD, TD, and control force criteria (α = 1, β = 1, V = 15 m/s)

Criteria	Hinf	PDa	PDd
$\ddot{z}_1$	-16.54	-63.97	-9.29
SD	-13.78	-2.15	-19.22
TD	7.62	-19.90	17.63
u	0	-4.62	-1.29

The time responses of the body acceleration, the relative SD, the relative TD, the relative TF, and the control force when V = 10 m/s and 15 m/s (α = 1, β = 1) are shown in Fig. 8 and Fig. 9, respectively.

The results in Tables 2 and 3 and Fig. 8 and Fig. 9 show that PDa is still effective in reducing the vehicle body acceleration and tyre deflection.

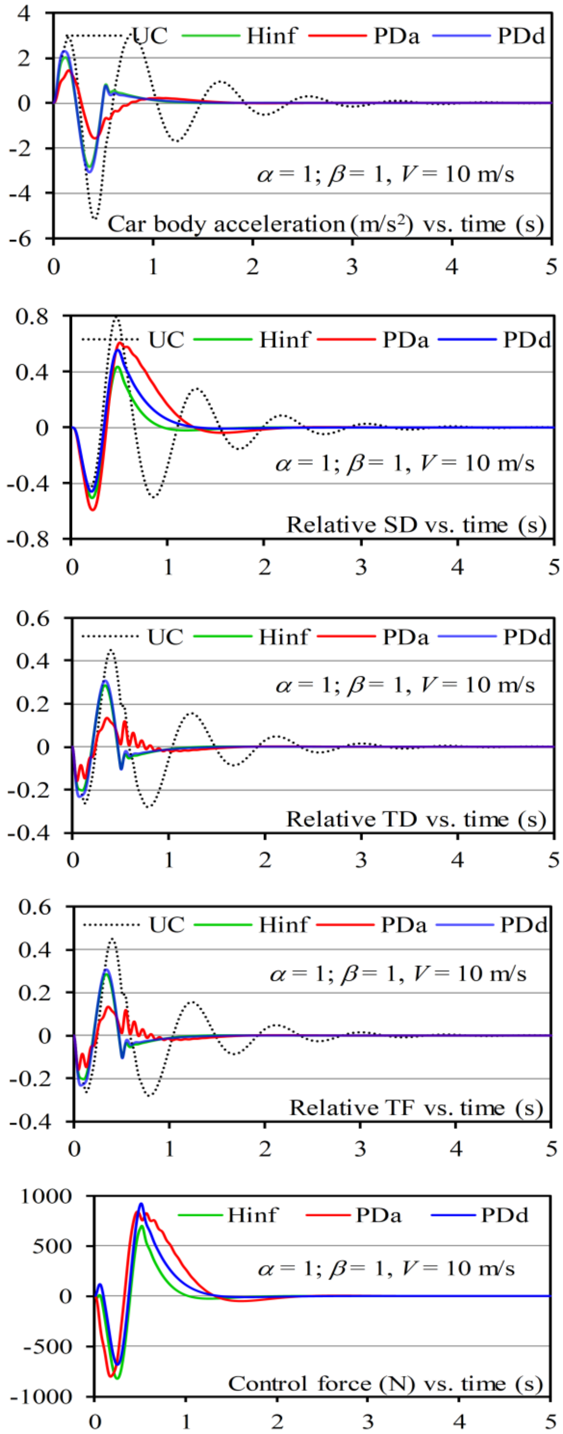

Fig. 8. The system's time responses in the case of α = 1 and β = 1, V = 10 m/s

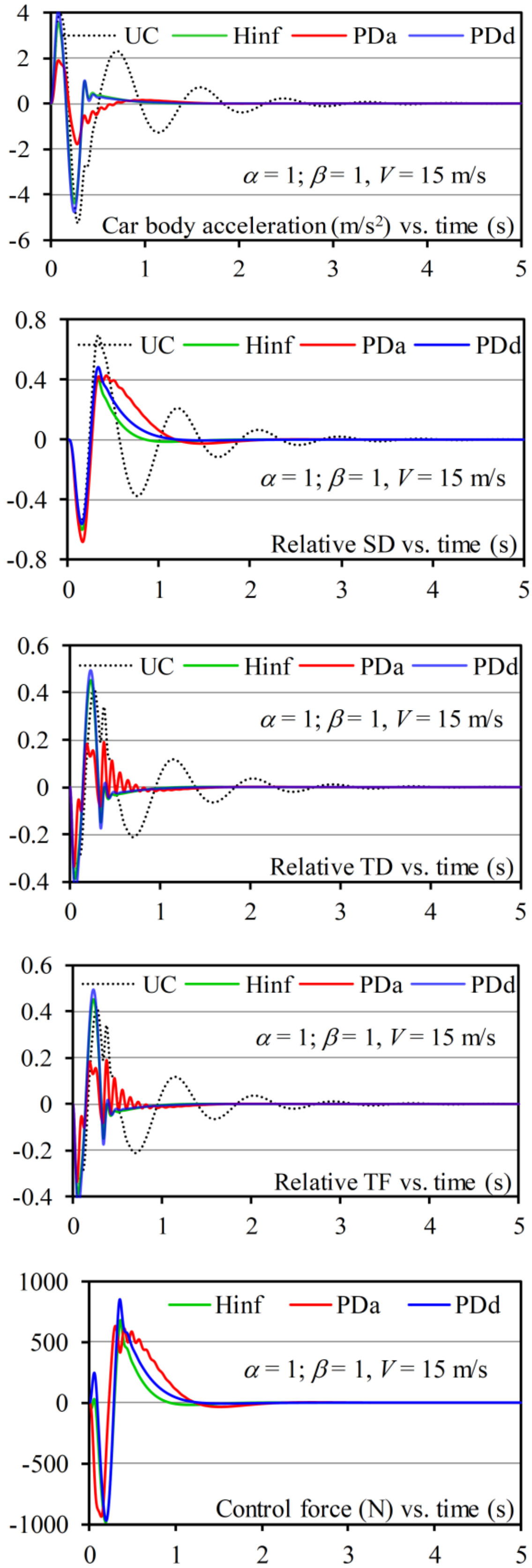

Fig. 9. The system's time responses in the case of α = 1 and β = 1, V = 15 m/s

5. Conclusion

This study presents an approach for the optimal design of PD controllers for the active suspension system of a quarter-car model. The setup steps of these controllers are simple and explicit based on optimizing the parameters of the gain vector using the BCMO algorithm. The proposed controllers are highly effective, especially for reducing the vehicle body acceleration by the PDa controller. The approach can be extended to active suspension models with more degrees of freedom and nonlinearity and to controlled mechanical models in general.

Acknowledgments

This research is funded by Vietnam National Foundation for Science and Technology Development (NAFOSTED) under grant number 107.01-2023.38.

References

[1] Z.R. Wani, M. Tantray, E.N. Farsangi, N. Nikitas, M. Noori, B. Samali, T. Yang, A Critical review on control strategies for structural vibration control, Annual Reviews in Control, vol. 54, pp. 103-124, 2022. https://doi.org/10.1016/j.arcontrol.2022.09.002

[2] N.-A. Tran, H.-L. Bui, Rolling tuned mass damper for vibration control of building structures subjected to earthquakes: a comparative study, Soil Dynamics and Earthquake Engineering, vol. 194, pp. 109376, 2025. https://doi.org/10.1016/j.soildyn.2025.109376

[3] K. Ghaedi, Z. Ibrahim, H. Adeli, A. Javanmardi, Invited review: recent developments in vibration control of building and bridge structures, Journal of Vibroengineering, vol. 19, iss. 5, pp. 3564-3580, Aug. 2017. https://doi.org/10.21595/jve.2017.18900

[4] O. El-Khoury, H. Adeli, Recent advances on vibration control of structures under dynamic loading, Archives of Computational Methods in Engineering, vol. 20, pp. 353-360, Oct. 2013. https://doi.org/10.1007/s11831-013-9088-2

[5] R. Kandasamy, F. Cui, N. Townsend, C.C. Foo, J. Guo, A. Shenoi, Y. Xiong, A Review of vibration control methods for marine offshore structures, Ocean Engineering, vol. 127, pp. 279-297, Nov. 2016. https://doi.org/10.1016/j.oceaneng.2016.10.001

[6] B. Fu, R.L. Giossi, R. Persson, S. Stichel, S. Bruni, R. Goodall, Active suspension in railway vehicles: a literature survey, Railway Engineering Science, vol. 28, pp. 3-35, Mar. 2020. https://doi.org/10.1007/s40534-020-00207-w

[7] A. Soliman, M. Kaldas, Semi-active suspension systems from research to mass-market - a review, Journal of Low Frequency Noise, Vibration and Active Control, vol. 40, iss. 2, pp. 1005-1023, Oct. 2019. https://doi.org/10.1177/1461348419876392

[8] J. Theunissen, A. Tota, P. Gruber, M. Dhaens, A. Sorniotti, Preview-based techniques for vehicle suspension control: a state-of-the-art review, Annual Reviews in Control, vol. 51, pp. 206-235, 2021. https://doi.org/10.1016/j.arcontrol.2021.03.010

[9] T. Le-Duc, Q.-H. Nguyen, H. Nguyen-Xuan, Balancing composite motion optimization, Information Sciences, vol. 520, pp. 250-270, May 2020. https://doi.org/10.1016/j.ins.2020.02.013

[10] W. Sun, H. Gao, P. Shi, Advanced Control for Vehicle Active Suspension Systems, Cham, Switzerland: Springer, 2020. https://doi.org/10.1007/978-3-030-15785-2

[11] T.-T. Mac, T.-D. Nguyen, H.-L. Bui, N.-A. Tran, Optimal design of hedge-algebras–based controller for vibration control of vehicle suspension systems, Proceedings of the Institution of Mechanical Engineers, Part I: Journal of Systems and Control Engineering, vol. 238, no. 4, pp. 755-776, Sep. 2023. https://doi.org/10.1177/09596518231196900